DNA Recognition

DOI: 10.1002/anie.200604294

Kinetic Recognition of AT-Rich DNA by Ruthenium Complexes**

*Pär Nordell, Fredrik Westerlund, L. Marcus Wilhelmsson, Bengt Nordén, and Per Lincoln**

DNA recognition, in nature as well as gene-targeting technology, is generally based on thermodynamically controlled equilibrium binding.[1–6] In the classical lock-and-key model, the DNA nucleobases, in close contact with the bound drug, determine the binding affinity, which limits selectivity to short sequences for small drug molecules. Herein we report that a high selectivity for long AT stretches can be attained through kinetically controlled DNA intercalation by binuclear ruthenium(II) complexes. The number of adjacent A–T base pairs is a decisive factor for the intercalation rate that is found to vary more than three orders of magnitude between mixed-sequence and alternating AT-sequence DNA. We speculate that this principle of kinetic recognition may be used by nature in nucleic acid biology. More specifically, kinetic recognition can be exploited to direct drugs to DNA targets characterized by long AT stretches in a highly selective manner.

The prototype DNA-binding ruthenium(II) complex $[Ru(phen)_3]^{2+}$ (phen = 1,10-phenanthroline) was introduced as a DNA conformation probe by Barton et al. in 1984. The propeller-shaped molecule binds by partial insertion of one phen ligand into the base-pair stack.[7,8] The right-handed Δ enantiomer prefers binding to mixed sequence and GC-rich DNA, whereas the left-handed Λ complex prefers AT-rich DNA, but the selectivity is modest.[9–11] Fusing a quinoxaline ring system to one of the phen ligands gives the complex $[Ru(phen)_2dppz]^{2+}$ (dppz = dipyrido[3,2-*a*;2′,3′-*c*]phenazine), which reveals much stronger DNA binding owing to intercalation of the extended ligand dppz. Δ-$[Ru(phen)_2dppz]^{2+}$ prefers binding to AT sites ($\Delta\Delta G^0 = -4.3$ kJ mol^{-1})[12] and has a slightly higher affinity when compared with the Λ enantiomer for binding to mixed-sequence (calf thymus) DNA ($\Delta\Delta G^0 = -1.6$ kJ mol^{-1}).[13] When the dppz ligand is shielded from water in the hydrophobic intercalation pocket, the complex becomes brightly luminescent ("molecular light switch").[14,15] The light-switch effect is also observed for the dimer **P**, which is obtained by connecting two $[Ru(phen)_2dppz]^{2+}$ complexes with a single bond, and for the corresponding 2,2′-bipyridine analogue **B** (Figure 1). Initially, **P** and **B** bind with high affinity in a nonluminescent binding mode on the outside of the DNA helix. A slow increase in luminescence then follows owing to intercalation of the bridging bidppz ligand by threading of one coordinated Ru^{2+} ion through the stack of DNA bases.[16–18]

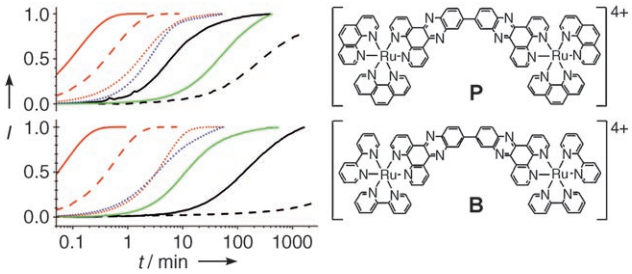

Figure 1. Kinetic discrimination between AT-rich and calf-thymus DNA. Intercalation kinetics of binuclear ruthenium complexes **P** (upper panel) and **B** (lower panel) at 50 °C (——), 37 °C (– – –), and 25 °C (•••••). Color coding: ΛΛ binding to poly(dAdT)$_2$ (red) and calf-thymus DNA (black); ΔΔ binding to poly(dAdT)$_2$ (blue) and calf-thymus DNA (green). Δ and Λ denote that the chirality of the propeller-like Ru coordination is right- and left-handed, respectively. The fraction of intercalated complex is determined as luminescence intensity normalized to its final value. With calf-thymus DNA at 37 °C, the final intensity was determined after a further 18 h at 50 °C. For poly(dAdT)$_2$, the curves at 37 °C and 50 °C were calculated by integration of the appropriate temperature-dependent rate law (see the Supporting Information). Complex structures to the right: $[\mu\text{-(bidppz)}X_4Ru_2]^{4+}$ with bidppz = 11,11′-bi(dipyrido[3,2-*a*:2′,3′-*c*]phenazinyl) and **X** = 1,10-phenanthroline (**P**) or **X** = 2,2′-bipyridine (**B**).

In contrast to the small variations in equilibrium binding affinity observed for the mononuclear ruthenium complexes, the DNA intercalation rate of the binuclear complexes strongly depends on the nucleobase composition of the DNA as well as on the structure and stereochemistry of the complex (Figure 1). Although both enantiomeric forms of the **P** and **B** complexes intercalate into poly(dAdT)$_2$ within a few minutes at 25 °C, their rates of intercalation into mixed-sequence DNA are very low even at 50 °C and show much greater variation. For the Δ enantiomers, we find that ΔΔ-**B** intercalates four times faster than ΔΔ-**P** (time to reach half completion, $t_{1/2} = 11$ min and 45 min, respectively). In the Λ series, on the contrary, ΛΛ-**B** intercalates 20 times slower than ΛΛ-**P** ($t_{1/2} = 132$ min and 6 min, respectively). Kinetic traces for the ΛΛ complexes intercalating into poly(dAdT)$_2$ at 50 °C could be obtained through extrapolation by using the Arrhenius equation (see the Supporting Information), which permits a comparison with calf-thymus DNA at this temperature. As can be seen from Figure 1, the slow rate of binding to mixed-sequence DNA makes ΛΛ-**B** outstandingly selective, and the ratio of $t_{1/2}$ for intercalation into calf-thymus DNA compared with poly(dAdT)$_2$ is estimated to be 2500 at 50 °C. The ratio is anticipated to be even larger at physio-

[*] P. Nordell, Dr. F. Westerlund, Dr. L. M. Wilhelmsson, Prof. B. Nordén, Dr. P. Lincoln
Department of Chemical and Biological Engineering/Physical Chemistry
Chalmers University of Technology
SE-412 96 Gothenburg (Sweden)
Fax: (+46) 31-772-3858
E-mail: lincoln@chalmers.se

[**] This work was supported by grants from the Swedish Research Council (VR).

Supporting information for this article is available on the WWW under http://www.angewandte.org or from the author.

logical temperatures as intercalation of ΛΛ-**B** into calf-thymus DNA is not complete even after 35 h at 37 °C.

Figure 2a shows emission intensities of ΛΛ-**B** after incubation at different temperatures with hairpin oligonucleotide duplexes with a central alternating AT tract of varying length (5′-CCGG**Y**GGCC-HEG-GGCC**Y**CCGG-3′, **Y** = $(AT)_3$, $(AT)_5$, $(AT)_7$, $(AT)_9$, or $(AT)_{11}$; HEG = hexaethylene glycol). Very low emission intensities for the shortest AT tract, **Y** = $(AT)_3$, show that ΛΛ-**B** does not intercalate even after long times at elevated temperatures. Increasing the length of the AT tract to 10 consecutive A–T base pairs (**Y** = $(AT)_5$) results in slow intercalation at a rate similar to that for calf-thymus DNA. Further lengthening of the AT tract leads to increasing intercalation rates, but as evident from the semilogarithmic plot in Figure 2c, the rate laws are not simple first order as for poly(dAdT)$_2$,[19] making quantitative comparisons difficult. As a rough measure, $t_{1/2}$ is about five times longer for **Y** = $(AT)_{11}$—that is, more than two complete helix turns of A–T base pairs—than for the polymer. Figure 2d shows emission traces at 25 °C of ΛΛ-**B** with poly(dAdT)$_2$, which has been pretreated by heating to 90 °C, followed by either slow annealing (giving back 97% duplex, as determined by UV absorption) or quick quenching in ice (73% duplex), compared with untreated polymer (100% duplex). Only a slight increase in the rate of intercalation (about 1.5 times) can be seen for the ice-quenched sample, which indicates that the number of bulges or hairpin structures present in the polymer repeat sequence is not a limiting factor for the rate of threading.

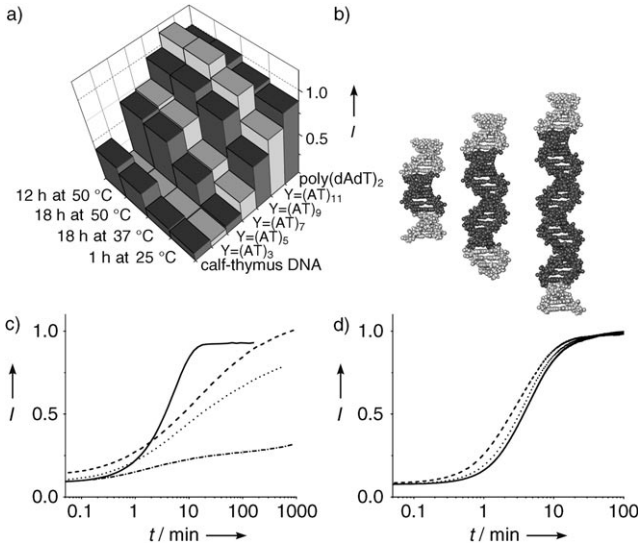

Figure 2. Fast threading intercalation of ΛΛ-**B** requires more than one helix turn of consecutive AT base pairs. a) Relative luminescence intensity of ΛΛ-**B** after incubation with calf-thymus DNA, five HEG-linked hairpin oligonucleotides of increasing AT content, or poly-(dAdT)$_2$. The data were collected after incubation at temperatures and times indicated. Luminescence normalized to the final intensity with poly(dAdT)$_2$. Oligonucleotide sequences: 5′-CCGG**Y**GGCC-HEG-GGCC**Y**CCGG-3′, where **Y** = $(AT)_n$. b) The hairpin oligonucleotide duplexes for **Y** = $(AT)_3$, $(AT)_7$, and $(AT)_{11}$ with AT tracts shaded in dark gray. c) Intercalation kinetics for ΛΛ-**B** to poly(dAdT)$_2$ (——) and oligonucleotides **Y** = $(AT)_7$ (–•–•), $(AT)_9$ (••••), and $(AT)_{11}$ (– – –) at 25 °C. d) Intercalation kinetics for ΛΛ-**B** to native (——), rapidly (– – –), or slowly (••••) annealed poly(dAdT)$_2$.

The first-order (**B**) or pseudo-first-order (**P**) kinetics found for intercalation of ΛΛ enantiomers into poly(dAdT)$_2$ make their energy barriers readily assessable.[19] As shown by the Arrhenius plot in Figure 3a, ΛΛ-**B** exhibits a dramatically higher activation energy (132 kJ mol^{-1}) than ΛΛ-**P** (97 kJ mol^{-1}) despite being sterically less hindered for passage through the DNA. The higher capability of phenanthroline, compared with bipyridine, to π stack with the nucleobases as observed in the [Ru(phen)$_3$]$^{2+}$ series[20] suggests that such interactions could also be important at the transition state for the threading of ΛΛ-**P**. As an illustration of this concept, a "minimal" transition state with only one open base pair is depicted in Figure 3c. One of the unpaired nucleobases is here energetically stabilized by stacking with the large planar phenanthroline in ΛΛ-**P**, thereby significantly lowering the

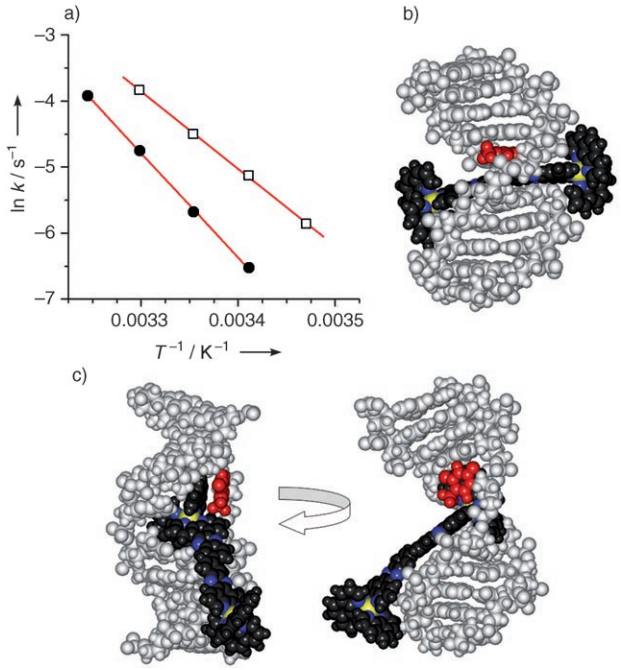

Figure 3. The bulkier ΛΛ-**P** has a lower activation energy for threading through DNA than ΛΛ-**B**. a) The Arrhenius plot of the rate constant for first-order threading kinetics gives E_a = 97 kJ mol^{-1} for ΛΛ-**P** (□) and E_a = 132 kJ mol^{-1} for ΛΛ-**B** (●). b) The final intercalative binding geometry of ΛΛ-**P** in $(AT)_6$ oligonucleotide duplex: bridging bidppz ligand sandwiched in the base-pair stack with one coordinated Ru^{2+} ion (yellow) in each groove of the double helix. c) Model of transition-state geometry for the threading process in which one coordinated Ru^{2+} ion is just about to pass through the helix centre. The extended planar structure of the phenanthroline ligands of ΛΛ-**P** promotes stacking with an unpaired base (red), thereby lowering the activation barrier by stabilizing the transition state. Model (b) was made by manual docking followed by energy minimization in the Amber force field in the HyperChem 5.1 program package. The transition state (c) was modeled by manually pulling out the binuclear complex towards the major groove in small steps allowing the system to relax adiabatically.

activation energy compared with the case with the smaller bipyridine in ΛΛ-**B**.

To determine if the complexes exhibit thermodynamic preference for poly(dAdT)$_2$, competition and dissociation experiments were performed. Figure 4a shows the emission spectra of an equilibrated sample of calf-thymus DNA and ΔΔ-**P** before and after incubation with poly(dAdT)$_2$ for 24 h at 50 °C compared with the spectrum in the presence of poly(dAdT)$_2$ alone. Complete redistribution to poly(dAdT)$_2$ shows that threading intercalation of ΔΔ-**P** indeed has a thermodynamic preference for long AT tracts. Similar results were obtained for the other three complexes (see Figure S2 in the Supporting Information). Figure 4b shows the luminescence decay after addition of sodium dodecyl sulfate (SDS) micelles at 50 °C, monitoring the dissociation of **P** and **B** from calf-thymus DNA and poly(dAdT)$_2$. As expected for threading intercalation, the rates are slow compared with the virtually instantaneous dissociation observed with common intercalating or groove-binding drugs.[21] Although the two ΔΔ enantiomers show similar rates of SDS sequestration for both types of DNA, the two ΛΛ enantiomers dissociate 5–10 times slower from poly(dAdT)$_2$ than from calf-thymus DNA, with ΛΛ-**B** showing the longest dissociation half-life of the four complexes (17 min; see Table S3 in the Supporting Information). It has recently been shown that dissociation rates determined by SDS sequestration are considerably overestimated for highly charged intercalators owing to catalysis by the surfactant and should therefore be interpreted with caution.[22,23] However, the much larger variation in the association kinetics suggests that the thermodynamic discrimination primarily reflects the differences in the rate of the forward process. This finding is in contrast with the anthracycline antibiotic nogalamycin, which binds by threading intercalation 50 times faster to poly(dAdT)$_2$ than to poly(dGdC)$_2$, but dissociates 160 times slower from the latter, leading to a thermodynamic GC selectivity.[21,24]

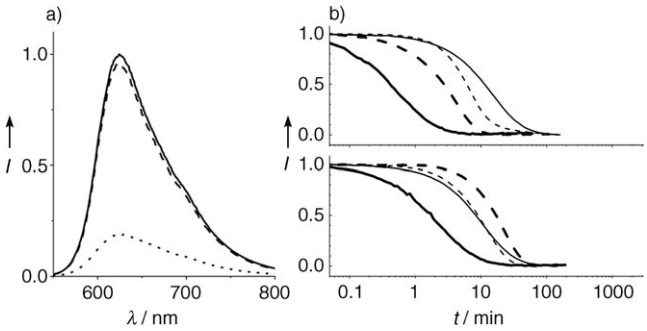

Figure 4. Binding competition and dissociation kinetics indicate a thermodynamic preference for poly(dAdT)$_2$. a) Competition binding. Emission spectra of ΔΔ-**P** intercalated in calf-thymus DNA (••••) and in poly(dAdT)$_2$ (——). An equivalent amount of poly(dAdT)$_2$ was added to the sample of calf-thymus DNA and incubated for 24 h at 50 °C. After correction for dilution, the resulting spectrum (– – –) is identical to that incubated with poly(dAdT)$_2$ only. b) Dissociation. Normalized luminescence change as a function of time after the addition of SDS to pre-equilibrated samples of **P** (top) and **B** (bottom) with calf-thymus DNA (——) and poly(dA-dT)$_2$ (– – –) at 50 °C (ΛΛ thick lines, ΔΔ thin lines). SDS concentration: 0.6% w/w.

Our results clearly demonstrate that kinetic recognition can provide a highly sequence-selective DNA interaction in which the selection mechanisms go beyond the short-range interactions of a simple lock-and-key model. Two kinds of effects are particularly worth noting: first, the requirement of more than one helix turn of AT base pairs for efficient threading intercalation (Figure 2), and, second, the high sensitivity of the rates to small geometric variations of the threading complexes (Figures 1, 3, and 4). The first effect indicates that the transition state involves a stretch of AT base pairs that is considerably larger than the dimensions of the intercalating complex itself. This suggests that a collective property, such as the duplex breathing dynamics, is a determining factor for the rate of threading. In mixed-sequence DNA, long AT stretches will be statistically rare, explaining the slow intercalation rates. The minor effect on the threading rate by not completely annealed poly(dAdT)$_2$ also indicates that it is the dynamics of the duplex, rather than entropically favored equilibrium base-pair defects, that lies behind the kinetic differences between the long AT-tract hairpin oligonucleotides and the polymer. The second kind of effect, in particular the decrease in the activation-energy barrier for the larger but more hydrophobic ΛΛ-**P**, shows that the intercalating molecule itself is intimately involved in the base-pair opening step.

Long stretches of very AT-rich sequences can be found in the genomes of some human pathogens, for example, in that of the malaria parasite *Plasmodium falciparum*.[26] The dynamic accessibility of long AT-rich DNA demonstrated herein may be of importance in the design of DNA-targeting drugs, and for the understanding of DNA interactions in nature.

Experimental Section

Experiments were conducted in 150 mM NaCl aqueous buffer solution (1 mM cacodylate, pH 7.0). For the time-based measurements, the polynucleotide (calf-thymus DNA and poly(dAdT)$_2$) [nucleobase] = 120 μM and [complex] = 3.75 μM. In the oligonucleotide experiments, [HEG-linked duplex] = 2 μM, [ΛΛ-**B**] = 2 μM, and polynucleotide [nucleobase] = 72 μM. Wavelengths: $\lambda_{ex} = 410$ nm, $\lambda_{em} = 650$ nm (time-based), $\lambda_{em} = 550$–800 nm (steady state). See the Supporting Information for experimental details.

Received: October 19, 2006
Revised: December 20, 2006
Published online: February 20, 2007

Keywords: DNA recognition · intercalation · kinetics · luminescence · ruthenium

[1] Y. Choo, A. Klug, *Curr. Opin. Struct. Biol.* **1997**, *7*, 117.
[2] C. Hélène, *Nature* **1998**, *391*, 436.
[3] S. White, J. W. Szewczyk, J. M. Turner, E. E. Baird, P. B. Dervan, *Nature* **1998**, *391*, 468.
[4] C. Bailly et al., *Biochemistry* **1994**, *33*, 15348; (see the Supporting Information).
[5] A. Abu-Daya, K. R. Fox, *Nucleic Acids Res.* **1997**, *25*, 4962.

[6] C. Bailly, R. K. Arafa, F. A. Tanious, W. Laine, C. Tardy, A. Lansiaux, P. Colson, D. W. Boykin, W. D. Wilson, *Biochemistry* **2005**, *44*, 1941.
[7] J. K. Barton, A. Danishefsky, J. Goldberg, *J. Am. Chem. Soc.* **1984**, *106*, 2172.
[8] P. Lincoln, B. Nordén, *J. Phys. Chem. B* **1998**, *102*, 9583.
[9] J. K. Barton, J. M. Goldberg, C. V. Kumar, N. J. Turro, *J. Am. Chem. Soc.* **1986**, *108*, 2081.
[10] C. Hiort, B. Nordén, A. Rodger, *J. Am. Chem. Soc.* **1990**, *112*, 1971.
[11] S. Satyanarayana, J. C. Dabrowiak, J. B. Chaires, *Biochemistry* **1993**, *32*, 2573.
[12] R. E. Holmlin, E. D. A. Stemp, J. K. Barton, *Inorg. Chem.* **1998**, *37*, 29.
[13] I. Haq, P. Lincoln, D. Suh, B. Nordén, B. Z. Chowdhry, J. B. Chaires, *J. Am. Chem. Soc.* **1995**, *117*, 4788.
[14] A. E. Friedman, J. C. Chambron, J. P. Sauvage, N. J. Turro, J. K. Barton, *J. Am. Chem. Soc.* **1990**, *112*, 4960.
[15] C. Hiort, P. Lincoln, B. Nordén, *J. Am. Chem. Soc.* **1993**, *115*, 3448.
[16] P. Lincoln, B. Nordén, *Chem. Commun.* **1996**, 2145.
[17] L. M. Wilhelmsson, F. Westerlund, P. Lincoln, B. Nordén, *J. Am. Chem. Soc.* **2002**, *124*, 12092.
[18] L. M. Wilhelmsson, E. K. Esbjörner, F. Westerlund, B. Nordén, P. Lincoln, *J. Phys. Chem. B* **2003**, *107*, 11784.
[19] P. Nordell, P. Lincoln, *J. Am. Chem. Soc.* **2005**, *127*, 9670.
[20] A. M. Pyle, J. P. Rehmann, R. Meshoyrer, C. V. Kumar, N. J. Turro, J. K. Barton, *J. Am. Chem. Soc.* **1989**, *111*, 3051.
[21] K. R. Fox, C. Brassett, M. J. Waring, *Biochim. Biophys. Acta* **1985**, *840*, 383.
[22] F. Westerlund, L. M. Wilhelmsson, B. Nordén, P. Lincoln, *J. Am. Chem. Soc.* **2003**, *125*, 3773.
[23] R. A. Marcus, *J. Phys. Chem. B* **2005**, *109*, 21419.
[24] K. R. Fox, M. J. Waring, *Biochim. Biophys. Acta* **1984**, *802*, 162.
[25] F. A. Tanious, S. F. Yen, W. D. Wilson, *Biochemistry* **1991**, *30*, 1813.
[26] M. J. Gardner et al., *Nature* **2002**, *419*, 498; (see the Supporting Information).

